

MI-0036

MAIN INJECTOR DIPOLE MAGNET:
2D FIELD COMPUTATIONS

JEAN-FRANÇOIS OSTIGUY

MI-0036

Main Injector Dipole Magnet: 2D Field Computations

Jean-François Ostiguy
AD/Accelerator Physics

October 1, 1990

1 Introduction

The purpose of this note is to document various calculations performed with the code PE2D. PE2D is a finite element code which solves for the vector potential in a 2D region. Compared to POISSON, a well-known code in the accelerator physics community, PE2D allows the user to create triangular meshes which are extremely dense only in the region of interest. The code employs second order isoparametric elements i.e., curvilinear triangles whose edges are second order curves over which the vector potential is interpolated by second order polynomials. The large system of equations which results from the discretization is solved using a state of the art algorithm (ICCG); for a given number of nodes, the results are more accurate than those produced by POISSON; furthermore, the CPU resources necessary to obtain a solution are considerably reduced.

2 Theory and Conventions

The magnetic field in a source free region can be derived from a scalar potential function which verifies Laplace's equation. In two dimensions, this scalar function can be seen as either the real or imaginary part of an analytic function $F(z)$. We therefore introduce a complex potential

$$F(z) = -A(x, y) - iV(x, y) \quad (1)$$

where $A(x, y)$ and $V(x, y)$ are respectively the magnetic scalar and vector potentials, from which the magnetic field is derived as follows:

$$\mathbf{B} = \frac{\partial A}{\partial z} \hat{x} - \frac{\partial A}{\partial x} \hat{y} \quad (2)$$

$$= -\frac{\partial V}{\partial x}\hat{x} - \frac{\partial V}{\partial y}\hat{y} \quad (3)$$

Using (2) and (3) it is easily verified that

$$\frac{dF}{dz} = B_y + iB_x \quad (4)$$

Furthermore, since $F(z)$ verifies the Cauchy-Riemann relations, it is analytic and so are all its derivatives. The complex potential $F(z)$ can be expanded as a Taylor series about the origin

$$F(z) = \sum_{n=0}^{\infty} c_n z^n \quad (5)$$

Thus

$$B_y + iB_x = \sum_{n=1}^{\infty} n c_n z^{n-1} \quad (6)$$

Using the polar representation of z and setting $c_n = b_n + ia_n$, (5) can be recast in the form

$$\begin{aligned} F(z) &= \sum_{n=0}^{\infty} (b_n + ia_n) \left(\frac{r}{r_0}\right)^n e^{in\phi} \quad (7) \\ &= \sum_{n=0}^{\infty} \left(\frac{r}{r_0}\right)^n [(b_n \cos n\phi - a_n \sin n\phi) + i(a_n \cos n\phi + b_n \sin n\phi)] \quad (8) \end{aligned}$$

where r_0 is a conveniently chosen normalization radius. Identifying the real and imaginary parts of (1) and (7) yields

$$A(r, \phi) = -\sum_{n=0}^{\infty} \left(\frac{r}{r_0}\right)^n (b_n \cos n\phi - a_n \sin n\phi) \quad (9)$$

$$V(r, \phi) = -\sum_{n=0}^{\infty} \left(\frac{r}{r_0}\right)^n (a_n \cos n\phi - b_n \sin n\phi) \quad (10)$$

$$B_y(r, \phi) = \sum_{n=1}^{\infty} \left(\frac{r}{r_0}\right)^{n-1} \frac{n}{r_0} [b_n \cos(n-1)\phi - a_n \sin(n-1)\phi] \quad (11)$$

$$B_x(r, \phi) = \sum_{n=1}^{\infty} \left(\frac{r}{r_0}\right)^{n-1} \frac{n}{r_0} [b_n \sin(n-1)\phi + a_n \cos(n-1)\phi] \quad (12)$$

The multipoles coefficients a_n and b_n can be obtained by expanding any one of the potentials or field components as a Fourier series in the angular variable ϕ .

For instance,

$$a_n = +\frac{1}{\pi} \int_0^{2\pi} \left(\frac{r_0}{r}\right)^n A(r, \phi) \sin n\phi \, d\phi \quad (13)$$

$$b_n = -\frac{1}{\pi} \int_0^{2\pi} \left(\frac{r_0}{r}\right)^n A(r, \phi) \cos n\phi \, d\phi \quad (14)$$

The geometry of a dipole magnet is usually such that $B_y(x, -y) = B(x, y)$ and $B_x(-x, y) = -B_x(x, y)$. The latter condition imposes $a_n = 0$ and the former $b_{2k} = 0$ $k = 1, 2, 3, \dots$. Since the vanishing of the a_n depends on a "top-bottom" symmetry which is usually present in most magnets (i.e., dipole, quads and sextupoles), the coefficients b_n and a_n are referred to as "normal" and "skew" respectively.

In particular, along the x -axis

$$B_y(x, 0) = \sum_{n=1}^{\infty} \frac{nb_n}{r_0} \left(\frac{x}{r_0}\right)^{n-1} \quad (15)$$

In practice, the radius used for the Fourier expansion must be as large as possible in order for the contribution of the higher order multipoles not to be lost in numerical noise. Nevertheless, r must be a bit smaller than the radius of convergence of the multipole expansion. The latter is equal to the shortest distance between the origin and the sources, i.e., magnetized material or current-carrying conductors. In this note, all multipoles are expressed in a system of coordinates where the radial coordinate is normalized at one inch i.e. 2.54 cm. The magnetic field is expressed in Tesla unless otherwise stated. The multipole coefficients are normalized with respect to the normal dipole field and therefore, have units of $\text{inch}^{-(n-1)}$ where $2n$ is the pole index. To avoid sign ambiguities, the dipole coefficient ¹ b_1 is always taken to be positive, which corresponds to a field pointing in the $+y$ direction. The signs of the higher order multipoles are to be interpreted relatively to the dipole coefficient.

3 Saturation and Field Quality

The most obvious way of generating a "constant" magnetic field is a simple "straight" gap such as the one shown in figure 1. Note the vertical profile which is meant to concentrate the flux in the gap region. Assuming for the moment that the permeability is infinite, it is intuitively clear that the vertical component of the field will have a tendency to decrease in magnitude as one moves away from the origin in the horizontal midplane. This effect, which can

¹The multipole index is often specified in reference to a power series expansion of the magnetic field rather than of the potential. In that case, b_0 is the dipole coefficient, b_1 is the quadrupole, b_2 is the sextupole, etc.

in the first approximation, be described by a negative sextupole term is usually compensated for by the introduction of small “bumps” or “shims” as illustrated in figure 2. By enhancing the vertical field at the edges of the magnet, the shims introduce a positive sextupole component. The compensation is usually such that the net sextupole is slightly positive. In practice, the permeability is a monotone decreasing function of the excitation. The magnitude of the dipole component of the field is slightly decreased due to the increased reluctance of the iron. The importance of the latter effect is often quoted in the form of a coefficient called AMPFAC (AMPere FACtor) which is simply the ratio between the dipole field corresponding to infinite permeability and the actual dipole field

$$\text{AMPFAC} = \frac{b_1(\mu = \infty)}{b_1} \quad (16)$$

For small levels of saturation, AMPFAC is a measure of the factor by which the excitation current must be multiplied for the magnet to produce an on-axis field equal to that produced with an idealized $\mu = \infty$ core. As the excitation is increased, the shims are the first regions of the magnet to go into saturation; thus, the sextupole coefficient starts from a small positive value, goes through zero and becomes negative when the maximum current is reached. This phenomenon is illustrated in figure 3 where $B > 1.7198$ Tesla in the dark regions. The current is $I = 9417$ A.

The residual multipoles due to saturation i.e., for a given lamination geometry, the difference between the $\mu = \infty$ multipoles and the multipoles calculated by taking into account the BH curve of the steel are very sensitive to the exact form of this BH curve at high excitations. For practical reasons, there is often no available experimental data at excitation levels beyond a few hundred Oersteds. One must therefore have recourse to some form of extrapolation. Three options are available:

- Linear extrapolation
- Total saturation beyond the last data point available
- Extrapolation based on a physical model of the behavior of the material at high field

The code POISSON uses linear extrapolation and PE2D assumes total saturation i.e. $dB/dH = 1$ beyond the last data point. Since the magnetization must reach a maximum value at very large excitations, it is clear that linear extrapolation is too optimistic; on the other hand the assumption of total saturation beyond the last point on the curve is certainly overly pessimistic.

Figure 4 is a plot of the BH curve for the ARMCO steel which will be used in the fabrication of the main injector dipole magnets. Figure 5 is a plot of the permeability as a function of the excitation beyond the last point in the curve of figure 4 for three different extrapolation methods. The solid curve,

which is probably the most realistic, has been obtained by using the so-called Frolich-Kennelly extrapolation formula

$$\frac{1}{4\pi M} = \frac{1}{4\pi H} + \frac{1}{4\pi M_s} \quad [\text{CGS}] \quad (17)$$

where M_s is the saturation magnetization and a is a coefficient which depends on the material. For ARMCO steel,

$$a \simeq 9.1118 \quad 4\pi M_s \simeq 19407$$

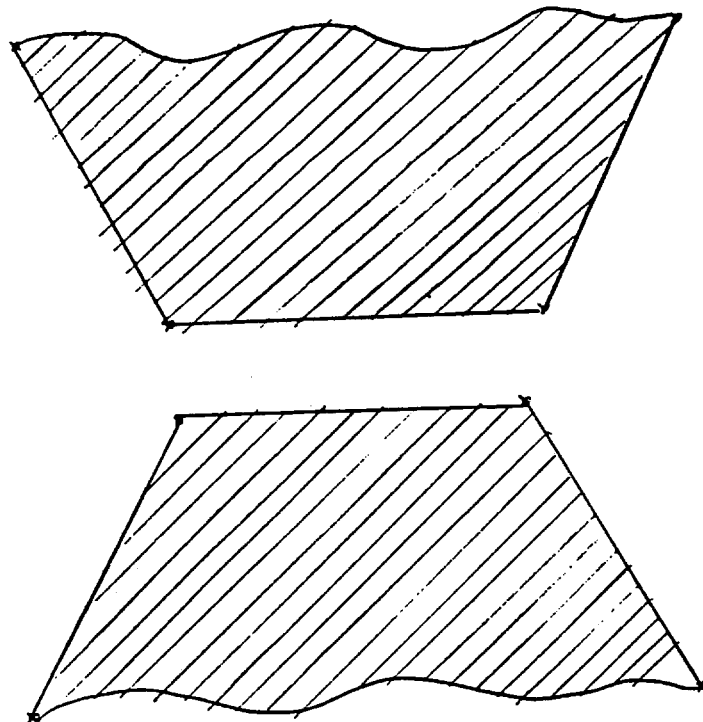


Figure 1: A simple "straight" gap.

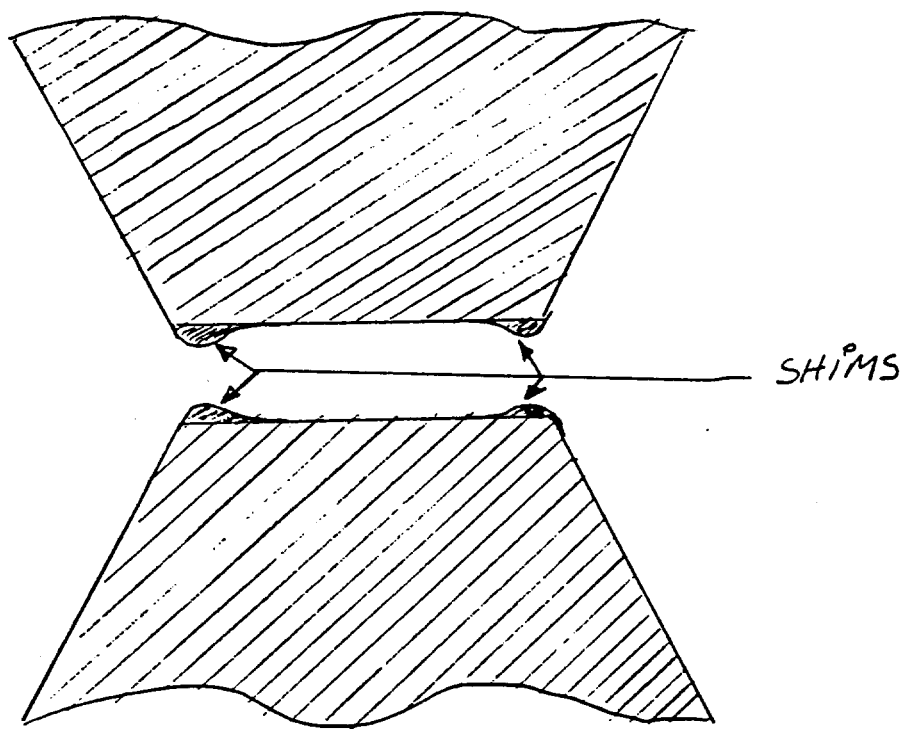


Figure 2: A corrected gap.

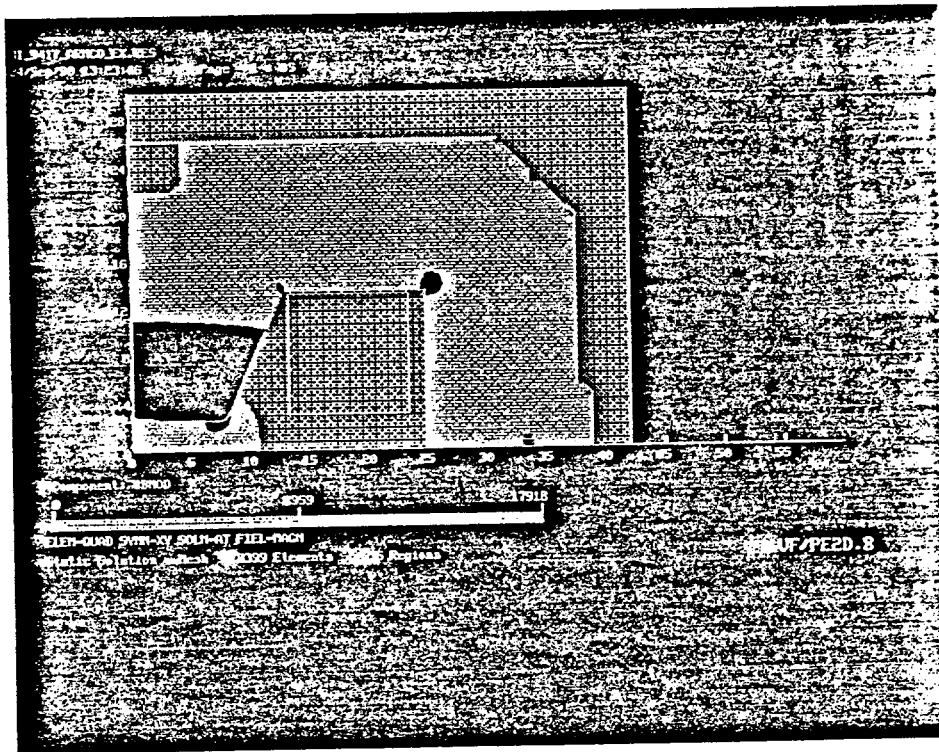


Figure 3: The tip of the pole and the correction shims are the first regions to saturate.

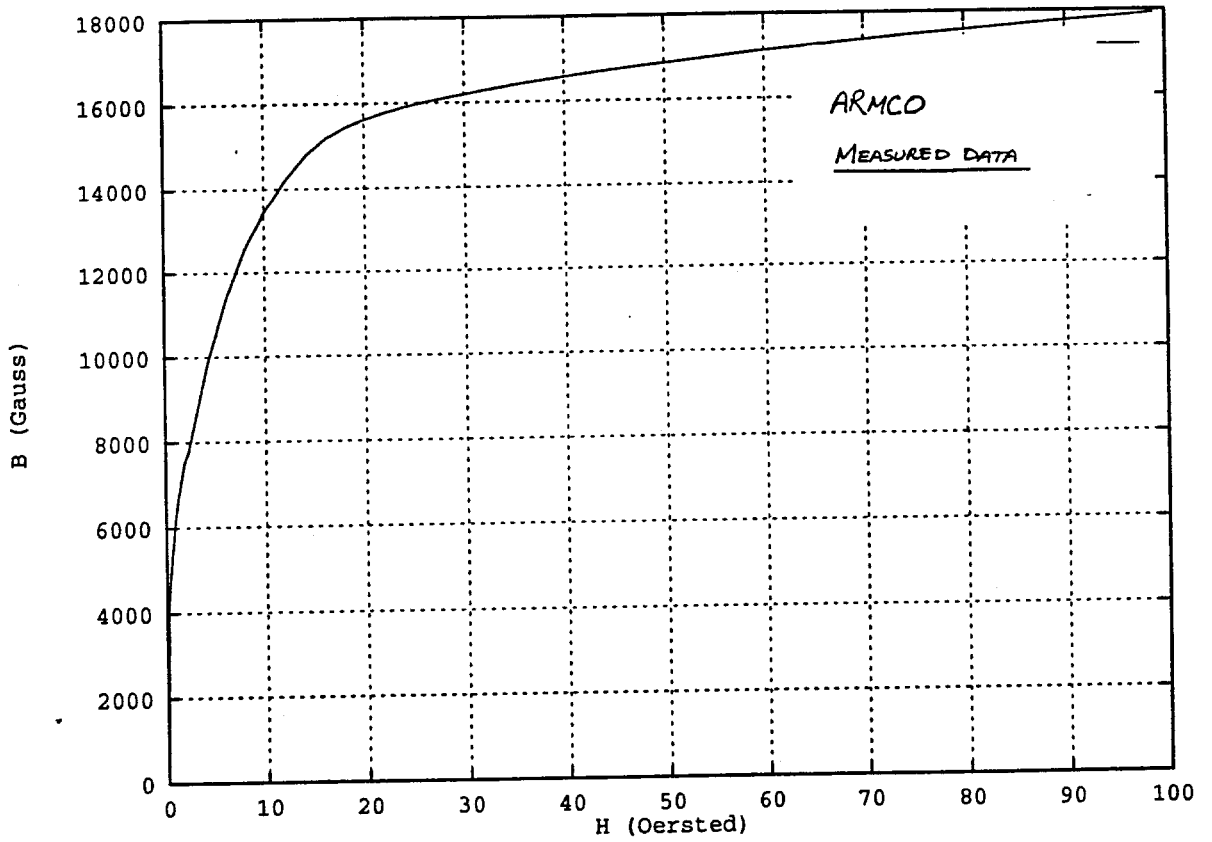


Figure 4: Experimental BH curve for the ARMCO magnetic steel used in the fabrication of the MI dipole magnet core.

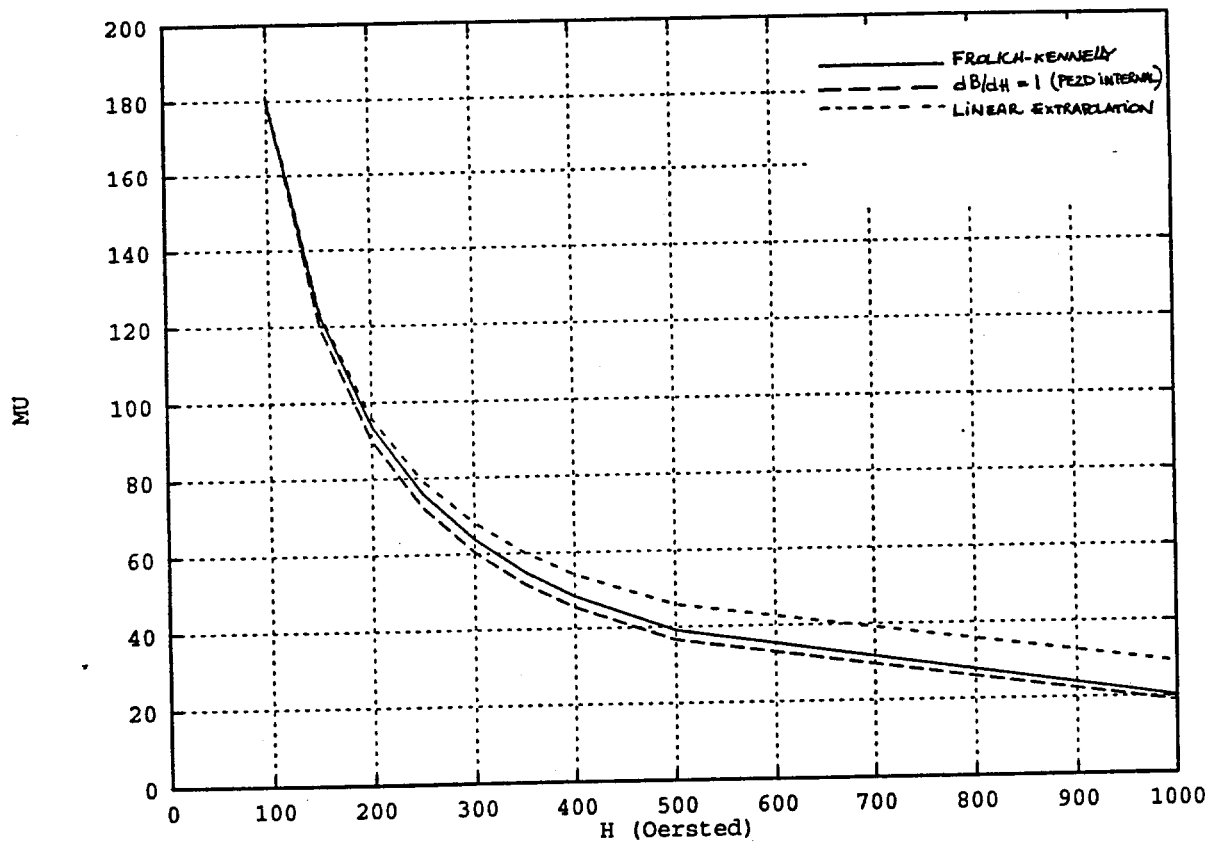


Figure 5: μ vs H at large H for three different extrapolation schemes.

<p style="text-align: center;">MAIN INJECTOR DIPOLE NORMAL MULTIPOLES AT $r = r_0 = 2.54$ cm INFINITE PERMEABILITY Dipole Field in Tesla Higher harmonics in relative units $\times 10^4$</p>	
	<p style="text-align: center;">$I = 9417$ A $J = 364.909$ A/cm²</p>
pole	
2	+1.86359
6	+0.21785
10	+0.17023
14	+0.03545

<p style="text-align: center;">MAIN INJECTOR DIPOLE NORMAL MULTIPOLES AT $r = r_0 = 2.54$ cm ARMCO steel laminations LINEAR EXTRAPOLATION Dipole Field in Tesla Higher Harmonics in relative units $\times 10^4$</p>				
	<p style="text-align: center;">$I = 502$ A $J = 19.4525$ A/cm²</p>	<p style="text-align: center;">$I = 4900$ A $J = 189.875$ A/cm²</p>	<p style="text-align: center;">$I = 7100$ A $J = 275.125$ A/cm²</p>	<p style="text-align: center;">$I = 9417$ A $J = 364.909$ A/cm²</p>
pole				
2	+0.09925	+0.96187	+1.38247	+1.73467
6	+0.22003	-0.02544	-0.97478	-9.24396
10	+0.18395	+0.15194	-0.04830	-1.29193
14	+0.04032	+0.00523	-0.01839	-0.15969

<p style="text-align: center;">MAIN INJECTOR DIPOLE NORMAL MULTIPOLES AT $r = r_0 = 2.54$ cm ARMCO steel laminations PE2D INTERNAL EXTRAPOLATION METHOD Dipole Field in Tesla Higher harmonics in relative units $\times 10^4$</p>				
	<p style="text-align: center;">$I = 502$ A $J = 19.4525$ A/cm²</p>	<p style="text-align: center;">$I = 4900$ A $J = 189.875$ A/cm²</p>	<p style="text-align: center;">$I = 7100$ A $J = 275.125$ A/cm²</p>	<p style="text-align: center;">$I = 9417$ A $J = 364.909$ A/cm²</p>
pole				
2	+0.09925	+0.96187	+1.38247	+1.686414
6	+0.22003	-0.02170	-0.97478	-22.05191
10	+0.18395	+0.15229	-0.04830	-7.89777
14	+0.04032	+0.01491	-0.01839	-0.53637

MAIN INJECTOR DIPOLE		
NORMAL MULTIPOLES AT $r = r_0 = 2.54$ cm		
ARMCO steel laminations		
FROLICH-KENNELLY EXTRAPOLATION METHOD		
Dipole Field in Tesla		
Higher harmonics in relative units $\times 10^4$		
	$I = 7100$ A $J = 275.125$ A/cm ²	$I = 9417$ A $J = 364.909$ A/cm ²
pole		
2	+1.38251	+1.72834
6	-1.02214	-14.5435
10	-0.08503	-3.34599
14	-0.02274	-0.46563

4 Effect of a Backleg gap

To facilitate the insertion of the coils, the main injector magnet core is constituted of two symmetric parts which are welded together in the final phases of the the assembly. Different factors, for example non-uniformities in the laminations may result in a small gap between the upper and lower sections of the core. To the extent that this gap is relatively uniform (or equivalently if the assembly errors are uniformly distributed along the length of the magnet), the principal effect of this "backleg" gap will be a small reduction in the magnitude of the dipole component of the field. Since they depend mostly on the pole profile, the higher order multipoles are not, in the first approximation, expected to be affected. In the case where the backleg gap is such that the left-right symmetry of the magnet is broken, one expects the appearance of even order coefficients. In the first approximation the most important effect is the appearance of a quadrupole term (b_2) in the multipole expansion of the field.

Multipoles have been calculated assuming both a symmetric and a wedge-shaped backleg gap as illustrated in figures 6 and 7 for $g = 0.0025, 0.0050, 0.025$ and $g = 0.050$ inch. As expected, except for a small reduction in the dipole, the odd order multipoles are not significantly affected by the presence of a backleg gap. On the other hand, a wedge-shaped gap introduces a significant quadrupole. As long as g remains small, the effect of the gap on both the dipole and the quadrupole coefficient scale linearly with g .

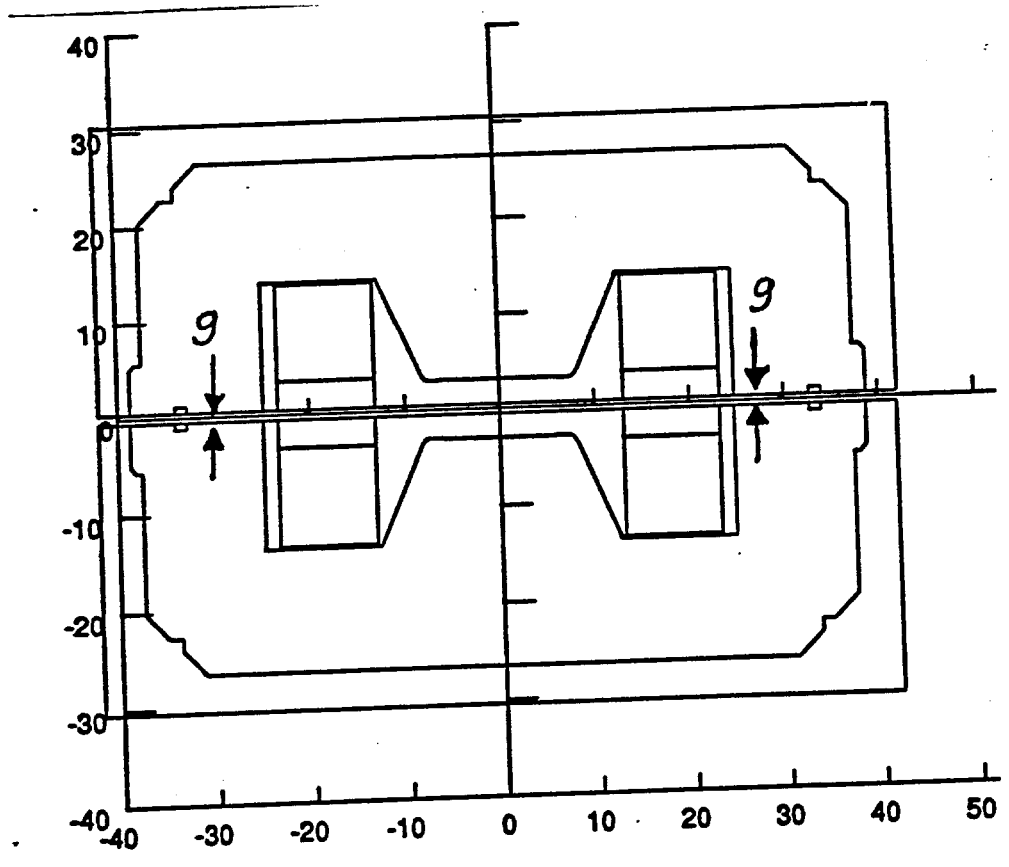


Figure 6: Symmetric backleg gap.

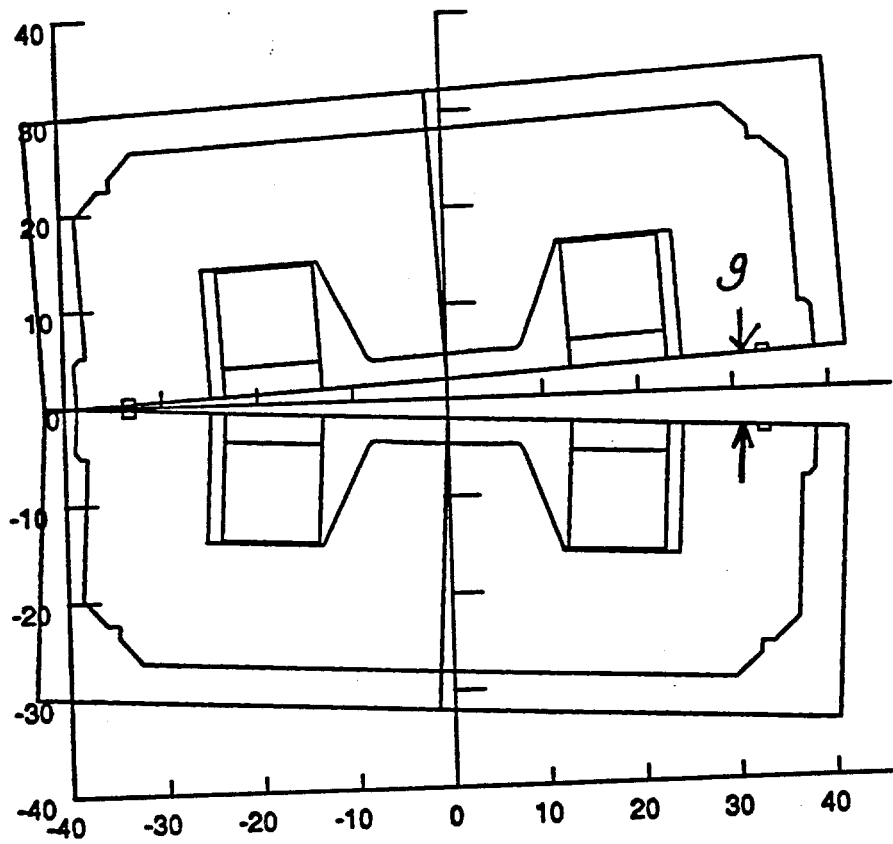


Figure 7: Wedge-shaped backleg gap.

NORMAL MULTIPOLES AT $r = r_0 = 2.54$ cm NO BACKLEG GAP - ARMCO steel laminations LINEAR EXTRAPOLATION Dipole Field in Tesla Higher harmonics in relative units $\times 10^4$			
	$I = 502$ A $J = 19.4525$ A/cm ²	$I = 4900$ A $J = 189.875$ A/cm ²	$I = 9417$ A $J = 364.909$ A/cm ²
pole			
2	+0.09925	+0.96188	+1.73755
4	+0.00000	+0.00000	+0.00000
6	+0.21726	-0.02391	-10.0010
8	+0.00000	+0.00000	+0.00000
10	+0.17684	+0.15729	-2.08174
12	+0.00000	+0.00000	+0.00000
14	+0.00332	-0.02691	-0.40160

NORMAL MULTIPOLES AT $r = r_0 = 2.54$ cm SYMMETRIC GAP 0.0025 in - ARMCO steel laminations LINEAR EXTRAPOLATION Dipole Field in Tesla Higher harmonics in relative units $\times 10^4$			
	$I = 502$ A $J = 19.4525$ A/cm ²	$I = 4900$ A $J = 189.875$ A/cm ²	$I = 9417$ A $J = 364.909$ A/cm ²
pole			
2	+0.09900	+0.95952	+1.73465
4	+0.00000	+0.00000	+0.00000
6	+0.21192	-0.04400	-9.93058
8	+0.00000	+0.00000	+0.00000
10	+0.16097	+0.13007	-2.08451
12	+0.00000	+0.00000	+0.00000
14	+0.02046	+0.02064	-0.41183

NORMAL MULTIPOLES AT $r = r_0 = 2.54$ cm SYMMETRIC GAP 0.0050 in - ARMCO steel laminations LINEAR EXTRAPOLATION Dipole Field in Tesla Higher harmonics in relative units $\times 10^4$			
	$I = 502$ A $J = 19.4525$ A/cm ²	$I = 4900$ A $J = 189.875$ A/cm ²	$I = 9417$ A $J = 364.909$ A/cm ²
pole			
2	+0.09876	+0.95717	+1.73174
4	+0.00000	+0.00000	+0.00000
6	+0.19791	-0.00459	-9.84453
8	+0.00000	+0.00000	+0.00000
10	+0.14862	+0.12645	-2.07478
12	+0.00000	+0.00000	+0.00000
14	+0.01785	+0.01968	-0.40761

NORMAL MULTIPOLES AT $r = r_0 = 2.54$ cm SYMMETRIC GAP 0.025 in - ARMCO steel laminations LINEAR EXTRAPOLATION Dipole Field in Tesla Higher harmonics in relative units $\times 10^4$			
	$I = 502$ A $J = 19.4525$ A/cm ²	$I = 4900$ A $J = 189.875$ A/cm ²	$I = 9417$ A $J = 364.909$ A/cm ²
pole			
2	+0.09683	+0.93879	+1.70864
4	+0.00000	+0.00000	+0.00000
6	+0.09982	-0.13618	-9.22067
8	+0.00000	+0.00000	+0.00000
10	+0.06631	+0.04919	-1.98676
12	+0.00000	+0.00000	+0.00000
14	-0.04725	-0.00734	-0.39189

NORMAL MULTIPOLES AT $r = r_0 = 2.54$ cm SYMMETRIC GAP 0.050 in - ARMCO steel laminations LINEAR EXTRAPOLATION Dipole Field in Tesla Higher harmonics in relative units $\times 10^4$			
	$I = 502$ A $J = 19.4525$ A/cm ²	$I = 4900$ A $J = 189.875$ A/cm ²	$I = 9417$ A $J = 364.909$ A/cm ²
pole			
2	+0.09453	+0.91678	+1.68007
4	+0.00000	+0.00000	+0.00000
6	-0.05213	-0.27885	-8.61512
8	+0.00000	+0.00000	+0.00000
10	-0.04184	-0.05204	-1.94984
12	+0.00000	+0.00000	+0.00000
14	-0.03502	-0.03170	-0.37895

NORMAL MULTIPOLES AT $r = r_0 = 2.54$ cm WEDGE GAP 0.0025 in - ARMCO steel laminations LINEAR EXTRAPOLATION Dipole Field in Tesla Higher harmonics in relative units $\times 10^4$			
	$I = 502$ A $J = 19.4525$ A/cm ²	$I = 4900$ A $J = 189.875$ A/cm ²	$I = 9417$ A $J = 364.909$ A/cm ²
pole			
2	+0.09907	+0.95947	+1.73444
4	-0.98804	-0.93528	-0.90472
6	+0.19848	-0.02633	-10.1994
8	-0.00232	-0.00697	-0.01546
10	+0.16921	+0.13586	-1.53210
12	-0.00733	-0.01262	+0.00734
14	+0.04557	+0.03140	-1.05515

NORMAL MULTIPOLES AT $r = r_0 = 2.54$ cm WEDGE GAP 0.005 in - ARMCO steel laminations LINEAR EXTRAPOLATION Dipole Field in Tesla Higher harmonics in relative units $\times 10^4$			
	$I = 502$ A $J = 19.4525$ A/cm ²	$I = 4900$ A $J = 189.875$ A/cm ²	$I = 9417$ A $J = 364.909$ A/cm ²
pole			
2	+0.09892	+0.96106	+1.72540
4	-1.91357	-1.87329	-1.73345
6	+0.23251	+0.11877	-8.90151
8	-0.02519	-0.00735	+0.05863
10	+0.17082	+0.14813	-1.13453
12	-0.04396	-0.02859	-0.09653
14	+0.05421	+0.04296	-0.08077

NORMAL MULTIPOLES AT $r = r_0 = 2.54$ cm WEDGE GAP 0.025 in - ARMCO steel laminations LINEAR EXTRAPOLATION Dipole Field in Tesla Higher harmonics in relative units $\times 10^4$			
	$I = 502$ A $J = 19.4525$ A/cm ²	$I = 4900$ A $J = 189.875$ A/cm ²	$I = 9417$ A $J = 364.909$ A/cm ²
pole			
2	+0.09782	+0.94085	+1.70771
4	-9.13513	-9.08181	-8.58062
6	+0.17763	-0.07220	-8.96406
8	+0.00613	-0.02263	+0.06225
10	+0.14424	+0.09846	-1.84632
12	-0.01792	-0.03190	-0.01005
14	-0.02118	+0.02758	-0.42501

NORMAL MULTIPOLES AT $r = r_0 = 2.54$ cm WEDGE GAP 0.050 in - ARMCO steel laminations LINEAR EXTRAPOLATION Dipole Field in Tesla Higher harmonics in relative units $\times 10^4$			
	$I = 502$ A $J = 19.4525$ A/cm ²	$I = 4900$ A $J = 189.875$ A/cm ²	$I = 9417$ A $J = 364.909$ A/cm ²
pole			
2	+0.09650	+0.92378	+1.67500
4	-17.8608	-17.8495	-16.9610
6	+0.12173	-0.11537	-7.95976
8	-0.07737	-0.03882	+0.08713
10	+0.06155	+0.02951	-1.70557
12	+0.06825	-0.04400	-0.03274
14	-0.08227	+0.00979	-0.32488

5 Conductor Positioning

It might be necessary in practice to slightly reposition the conductors relatively to the magnet core in order to make room for insulation and cooling. Since the field quality is dictated mostly by the core geometry and its saturation behavior, it is not expected to be very sensitive to conductor position. Nevertheless, calculations have been performed to verify the validity of this assertion. In the first case, all four conductors have been moved vertically toward and horizontally away from the axis by 0.030 inch for each pole. This is illustrated in figure 8. In the second case, only the top left conductor has been displaced horizontally by 5.0 mm from its nominal position as shown in figure 9. Note that due to the breaking of both the left-right and top-bottom symmetries, all multipoles are non-zero in that case.

As expected, the calculations confirm that moving the conductors does not result in any significant degradation of the field quality.

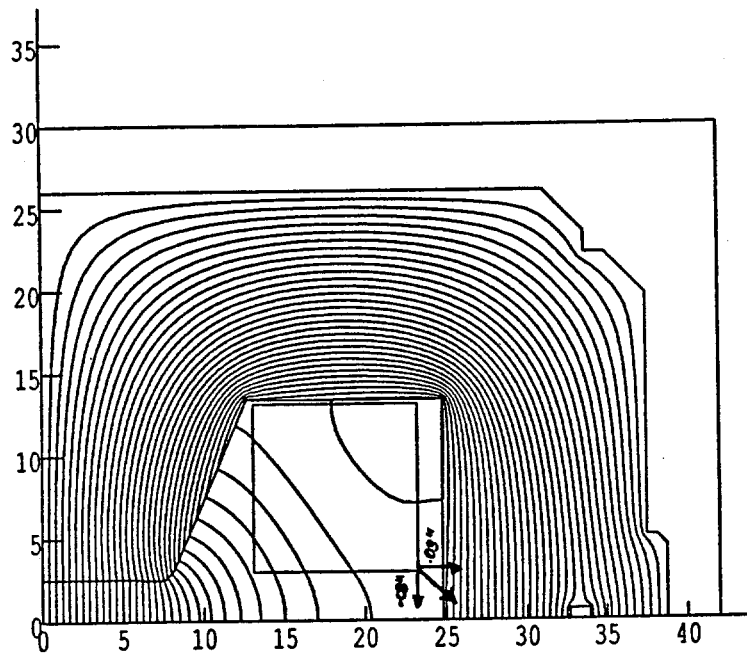


Figure 8: All four conductors are moved vertically toward the axis and horizontally away from the beam axis, symmetrically for each one of the four poles.

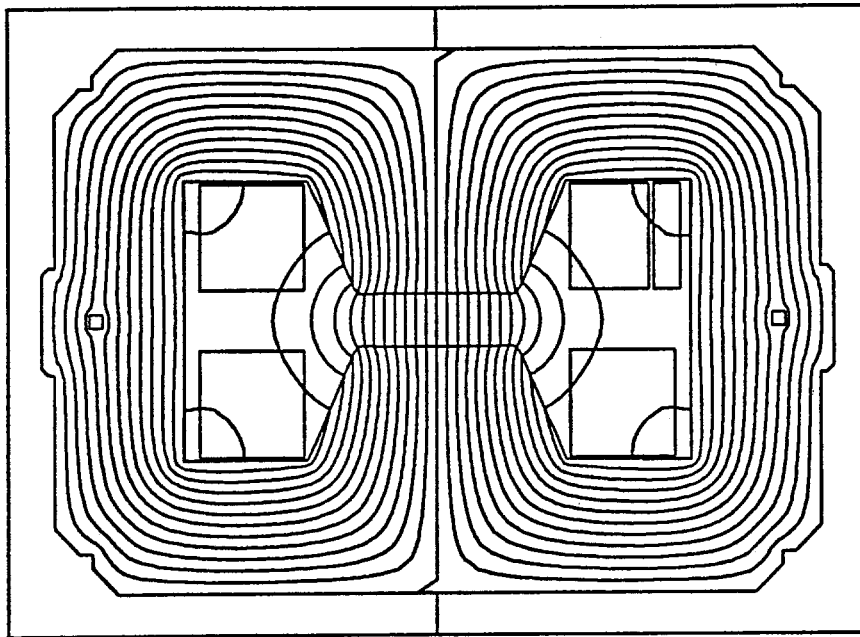


Figure 9: Only the top leftmost conductor is displaced horizontally.

NORMAL MULTIPOLES AT $r = r_0 = 2.54$ cm ARMCO steel laminations LINEAR EXTRAPOLATION Dipole Field in Tesla Higher harmonics in relative units $\times 10^4$				
		$I = 4900$ Amperes $J = 189.875$ A/cm ²	$I = 9417$ Amperes $J = 364.909$ A/cm ²	
pole	no offset	0.03 in offset	no offset	0.03 in offset
2	+0.961877	+0.961971	+1.734690	+1.734860
6	-0.000023	-0.000012	-0.016009	-0.016026
10	+0.000140	+0.000157	-0.002262	-0.002236
14	+0.000031	+0.000039	-0.000275	-0.000251

NORMAL MULTIPOLES AT $r = r_0 = 2.54$ cm ARMCO steel laminations LINEAR EXTRAPOLATION Dipole field in Tesla Higher harmonics in relative units $\times 10^4$				
		$I = 4900$ Amperes $J = 189.875$ A/cm ²	$I = 9417$ Amperes $J = 364.909$ A/cm ²	
pole	no offset	5 mm offset	no offset	5 mm offset
2	+0.96190	+0.96190	+1.73400	+1.73400
4	-0.00197	+0.00404	-0.00003	+0.00060
6	-0.01616	-0.01462	-9.27340	-9.26750
8	-0.00102	+0.00181	-0.00296	-0.00819
10	+0.16124	+0.15844	-1.19781	-1.20473
12	+0.00158	-0.00410	-0.00106	+0.00037
14	+0.03011	+0.03763	-0.29752	-0.30150

SKEW MULTIPOLES AT $r = r_0 = 2.54$ cm				
ARMCO steel laminations				
LINEAR EXTRAPOLATION				
Normal dipole field in Tesla				
Higher harmonics in relative units $\times 10^4$				
		$I = 4900$ Amperes $J = 189.875$ A/cm ²		$I = 9417$ Amperes $J = 364.909$ A/cm ²
pole	no offset	5 mm offset	no offset	5 mm offset
2	+0.00029	+0.00797	+0.00110	+0.03616
4	-0.00493	+0.00906	+0.00103	+0.03114
6	+0.00166	+0.00808	-0.00173	+0.01531
8	-0.00005	+0.00611	-0.00277	+0.01107
10	+0.00447	+0.00489	-0.00010	+0.00897
12	+0.00155	+0.00595	+0.00560	+0.00393
14	-0.00130	+0.00025	+0.00192	+0.00489

5. Summary

In short, it has been found that the beampipe will never melt as a consequence of the beam striking it at some small incident angle. With reasonable parameters for the energy deposited by the beam and the thermal characteristics of the steel pipe, a maximum temperature is reached which is approximately $400 \rightarrow 550$ °C below the melting point of the steel. At this point the energy dispersed through diffusion, convection, and radiation cancels the energy deposited by the beam.